Elsevier Editorial System(tm) for Journal of Crystal Growth
Manuscript Draft

Manuscript Number:

Title: Nucleation statistics in vapor-liquid-solid nanowires

Article Type: SI: ICCGE-17

Section/Category: General subjects

Keywords: A1 Nucleation, B1 Nanomaterials

Corresponding Author: Dr. Nickolay Vladimirovich Sibirev, Ph.D.

Corresponding Author's Institution: Saint-Petersburg Academic University

First Author: Nickolay Vladimirovich Sibirev, Ph.D.

Order of Authors: Nickolay Vladimirovich Sibirev, Ph.D.; Vladimir G Dubrovskii, Dr; Maxim V Nazarenko, Ph.D. ; Dagou A Zeze, Dr

Abstract: The statistics of nucleation events in nanowires growing via the vapor-liquid-solid mechanism in the mononuclear regime is studied theoretically. A semi-analytical model is developed which is capable of describing the distributions of time intervals between the successive nucleation events and some other useful characteristics of nucleation statistics. Very importantly, our model accounts for desorption from the droplet, which was not included in the previous studies. It is shown that the relative dispersion of nucleation distributions increases with the nanowire radius and at a higher desorption rate from the droplet, leading to the corresponding broadening of the length distribution. Using the model is also shown to fit well experimental data available on nucleation statistics in the Au-catalyzed Si and III-V nanowires.

***Highlights (for review)**

We proposed theoretical model of nucleation during the VLS growth of nanowires in the mononuclear regime

The model accounts for desorption from the droplet and allows one to describe the nucleation statistics and the nanowire length distribution.

It was shown that the relative dispersion of nanowire length increases with the NW radius and at a higher desorption from the droplet.

*Abstract

Abstract

The statistics of nucleation events in nanowires growing via the vapor-liquid-solid mechanism in the mononuclear regime is studied theoretically. A semi-analytical model is developed which is capable of describing the distributions of time intervals between the successive nucleation events and some other useful characteristics of nucleation statistics. Very importantly, our model accounts for desorption from the droplet, which was not included in the previous studies. It is shown that the relative dispersion of nucleation distributions increases with the nanowire radius and at a higher desorption rate from the droplet, leading to the corresponding broadening of the length distribution. Using the model is also shown to fit well experimental data available on nucleation statistics in the Au-catalyzed Si and III-V nanowires.

*Manuscript
Click here to view linked References

Nucleation statistics in vapor-liquid-solid nanowires

N.V. Sibirev[a,b*], M.V. Nazarenko[a,c], D.A. Zeze[d] and V.G. Dubrovskii[a,b,c]

[a] St. Petersburg Academic University, 194021, Russia

[b] St. Petersburg State University, 199034, Russia

[c] Ioffe Physical Technical Institute of the Russian Academy of Sciences, 194021, St. Petersburg , Russia

[d] School of Engineering and Computing Sciences, Durham University, DH1 3LE, UK

*Corresponding author

e-mail: NickSibirev@yandex.ru

Abstract

The statistics of nucleation events in nanowires growing via the vapor-liquid-solid mechanism in the mononuclear regime is studied theoretically. A semi-analytical model is developed which is capable of describing the distributions of time intervals between the successive nucleation events and some other useful characteristics of nucleation statistics. Very importantly, our model accounts for desorption from the droplet, which was not included in the previous studies. It is shown that the relative dispersion of nucleation distributions increases with the nanowire radius and at a higher desorption rate from the droplet, leading to the corresponding broadening of the length distribution. Using the model is also shown to fit well experimental data available on nucleation statistics in the Au-catalyzed Si and III-V nanowires.

Keywords: A1 Nucleation, B1 Nanomaterials

I. Introduction

Semiconductor nanowires (NWs) are one-dimensional nanocrystals with a high crystal quality and well-controlled properties which show a great potential for use in nanoelectronics [1], nano-optics [2] and nanosensing [3,4]. These NWs are usually grown via the vapor–liquid–solid (VLS) mechanism with a metal catalyst, where the nucleation of

nanowire monolayers (MLs) from a supersaturated alloy in the liquid droplet plays a crucial role [5-15]. The key effect underlying the VLS mechanism of NW growth is the decrease of the nucleation barrier on the NW top facet with respect to the case of a thin film without a catalyst [5, 6, 15]. The nucleation process determines the NW morphology [16-18], crystal structure [7, 12, 15, 19, 20], doping profiles [21, 22], and abruptness of heterointerfaces [23]. From a fundamental viewpoint, the VLS growth of NWs presents an interesting example of nucleation in nanovolumes [10, 14, 24].

As commonly assumed, VLS NWs grow layer-by-layer [7, 11, 25, 26]. Furthermore, sufficiently narrow NWs form in the so-called mononuclear regime where only one two-dimensional (2D) island nucleates in each layer and then rapidly spreads to fill the complete ML slice [14, 25, 27]. Most theoretical models consider VLS growth of NWs as a steady-state process at a time-independent supersaturation [5, 6, 9, 17, 28]. In this case, 2D nucleation events occur randomly and independently of each other [10, 14, 29]. This should lead to the Poissonian distribution over the NW lengths, which broadens very rapidly with growth time. However, such distributions are not observed experimentally: in fact, most NW length distributions are remarkably uniform [14].

To explain the observed length uniformity, one should assume a certain anti-correlation between the successive nucleation events that result in a sub-Poissonian length distribution [10]. This anti-correlation behavior is explained by the depletion of semiconductor material in the droplet after each nucleation event [10, 14, 15]. Indeed, as one ML is removed from the droplet, the latter appears nearly emptied with its semiconductor material and should be refilled again before the next ML can nucleate. When 2D island growth is much faster than the waiting time between the successive nucleation events, liquid supersaturation exhibits a sawtooth oscillatory behavior with time [15]. While there is no way to directly measure the time-dependent supersaturation during growth, its oscillatory behavior

has been demonstrated indirectly [10, 24, 30]. Such an anti-correlation is specific only for significantly small droplets: the narrowing effect gradually disappears as the droplet size increases [29].

This paper is devoted to a detailed theoretical description of nucleation statistics during the VLS growth of NWs in the mononuclear regime. We aim at a more precise description of individual nucleation events in the VLS NWs with accounting for the following kinetic processes: direct impingement, desorption and nucleation at the liquid-solid interface. To ascertain its validity, the model is then applied to a quantitative description of some relevant literature experimental data on Si [24] and III-V [10] NWs.

II. Model

Within the model, we assume that the incoming flux a impinging the droplet is independent of time, but equal to the product of the deposition rate J and the NW cross-section area πR^2, where R is the NW radius. For simplicity, the diffusion flux from the NW sidewalls is not considered here since it is not critical to the formulation of current model (although the corresponding generalization is straightforward [14]). The normalized evaporation flux from the droplet d equals N/τ, where N is the number of atoms within the material of interest dissolved in the droplet and τ is the effective lifetime in the liquid phase.

Assuming that the nucleation probability is entirely determined by the number of "semiconductor" (Si the case of Si NWs or As in the case of GaAs NWs) feeding atoms dissolved in the droplet at a given time. After the nucleation event occurs, the supercritical nucleus spreads almost instantaneously to fill the complete ML slice, as discussed above. Therefore, one can assume that the time needed to fill the ML is much shorter than the refill time [10, 14, 29]. Let V be the average growth rate of a NW and N^* the mean number of feeding atoms in the droplet that corresponds to the growth rate V. We then introduce the

deviation of the actual number of atoms in the droplet from the mean value according to $n=N-N^*$, referred to as the number of atoms in the droplet for brevity). Due to a very steep exponential dependence of the nucleation probability density $p(n)$ on the number of atoms n, the $p(n)$ can be put as [6, 14, 29]

$$p(n) \cong V \exp(\varphi n). \tag{1}$$

Here, φ is of the order of magnitude with the number of atoms in the critical nucleus divided to the equilibrium number of semiconductor atoms in the droplet at a given temperature and for a given NW radius: $\varphi \approx i_c / N_{eq} \propto R^{-3}$. The φ value scales with R^{-3} because N_{eq} is proportional to the droplet volume (R^3).

The kinetic equation describing the time dependence of the number of feeding atoms in the droplet can be expressed as

$$\frac{dn}{dt} = b - \frac{n}{\tau} - M\frac{dl}{dt}. \tag{2}$$

where, $b = a - N_* / \tau$ is the difference between the incoming and desorption fluxes, both corresponding to the mean number of feeding atoms N^*. M is the number of atoms in one ML of the NW, and dl/dt is the appropriately normalized vertical growth rate. The n value increases steadily between the two successive nucleation events. Assuming that n equals η at zero time (t=0), one can write down the equation describing the time evolution of n before the next nucleation event:

$$n = b\tau - (b\tau - \eta)\exp(-t/\tau). \tag{3}$$

Equations (1) and (3) allows us to find the conditional probability $q(x,n)$ of forming the next ML at a time x if the initial number of feeding atoms (at time zero) was n. since $dq/dx=p(1-q)$, the conditional probability is given by:

$$q(x,n) = 1 - \exp\left(-V\tau \exp(\varphi b\tau)\left[Ei(\varphi(n-b\tau)) - Ei(\varphi(n-b\tau)\exp(-x/\tau))\right]\right), \tag{4}$$

with $Ei(z)=\int_{-\infty}^{z}\frac{\exp(y)}{y}dy$ as the integral exponent. By definition, the probability density $s(x,n)$ of forming a ML exactly at the time x is given by $s(x,n)=dq(x,n)/dx$. To obtain the distribution of the time intervals between the successive nucleation events over time $T(x)$, the distribution over concentrations just before the nucleation event $U(n)$ must be known. At a given $U(n)$, the equation for $T(x)$ becomes

$$T(x)=\int_{-\infty}^{+\infty}U(n)s(x,n-M)dn. \tag{5}$$

In turn, the $U(n)$ distribution can be obtained from the probability $C(n)$ that the number of feeding atoms equals n at any time during growth (the concentration distribution), and the $p(n)$ distribution defined by Eq. (1):

$$U(n)=\frac{C(n)p(n)}{\int_{-\infty}^{+\infty}C(n)p(n)dn}=U_0C(n)\exp(\varphi n), \tag{6}$$

with the known U_0.

With these considerations, the problem is reduced to finding the concentration distribution $C(n)$. Here, we propose the following model equation for $C(n)$:

$$\left(b-\frac{n}{\tau}\right)\frac{d}{dn}C(n)-\frac{1}{\tau}C(n)=V\exp(\varphi(n+M))C(n+M)-V\exp(\varphi n)C(n). \tag{7}$$

The left hand side of this equation corresponds to the time evolution of the concentration distribution in absence of any nucleation events. If no nucleation occurs, the number of atoms in the droplet would approach its steady state value $b\tau$. The expression on the right hand side accounts for the discrete nucleation events that instantaneously remove M atoms from the droplet. This term has the form of a discrete rate equation, where the number of nucleation events per unit time is proportional to $p(n')C(n')$. Nucleation of a ML at $n'=n$ necessarily decreases the probability $C(n)$, while removing a ML at $n'=n+M$ retains the droplet to the

state with n atoms. Since Eq. (7) is a difference-differential equation, the boundary conditions must be imposed, i.e. not in a discrete point, but within an interval having the length M [31]. As a result, the number of atoms in the droplet can never exceed $b\tau$ due to desorption. Therefore, the value of $C(n)$ must be set to zero for any $n>b\tau$. However, the singular point $n=b\tau$ allows for an additional degree of freedom, which is determined by the normalization condition for $C(n)$. These conditions could be expressed as:

$C(n) \equiv 0$ for $n > b\tau$;

$$\int_{-\infty}^{b\tau} C(n)dn = 1. \tag{8}$$

Let us now consider the situation where the parameter φ is large enough to suppress temporally independent nucleation events, i.e., $\varphi M >> 1$. In this case, the solution to Eq. (7) can be approximated as:

$$C(n) = \exp\left(\frac{1}{n_\alpha \varphi}\left[\varphi(n+\Delta_V) - \exp(\varphi(n+\Delta_V))\right]\right)\left[1 - \exp\left(-\frac{1}{\varphi}\exp(\varphi(n+\Delta_M))\right)\right], \tag{9}$$

where $\Delta_V = \frac{1}{\varphi}\ln(V\tau)$, $\Delta_M = \frac{1}{\varphi}\ln(V\tau) + M - \varepsilon$, $\varepsilon = \frac{1}{\varphi}\ln\left(n_\alpha + \frac{M}{2} - \frac{1}{\varphi}\ln(n_\alpha \varphi)\right)$, and $n_\alpha = \frac{1}{\varphi}\ln(\alpha) = \frac{1}{\varphi}\ln(V\tau) + b\tau$. It can be seen that the non-vanishing part of the concentration distribution lies within the interval from $-\Delta_M + \ln\varphi/\varphi$ to $-\Delta_V + 3\ln(n_\alpha\varphi)/\varphi$. For very large values of φM , the distribution is concentrated within a narrow interval [-M,0] corresponding to a negative n. This means that number of atoms in the droplet exhibits a sawtooth oscillatory behavior similar to that described elsewhere [24].

Figure 1 shows the profiles of $C(n)$ distributions obtained from Eq. (9) at $V = 4$ ML/s, $\tau = 1$ s, $b = 2\times10^5$ s^{-1}, $N_{eq} = 5\times10^5$, $M = 5\times10^4$ and different φ varying from 5×10^{-5} to 1×10^{-2}, yielding the values of φM from 2.5 to 500. The distributions $C(n)$ lays within the

interval [-M,0] for large $\varphi \geq 4\times10^{-4}$. For smaller φ, the concentration distribution is more Poissonian-like, where the probability of having more than $b\tau$ atoms becomes non-zero.

To obtain the distribution over concentrations just before the nucleation event, one needs to consider only the right tail of the distribution *C(n)*. Indeed, the behavior of *C(n)* at negative *n* is insignificant, since it is zeroed by a rapidly decreasing $p(n)$ as given by Eq. (1). As a result, Eq. (6) may be re-written in the simplified form using Eq. (9):

$$U(n) = U_0 \exp(-\varphi n)\exp\left(\frac{1}{n_\alpha \varphi}\left[\varphi(n+\Delta_V) - \exp(\varphi(n+\Delta_V))\right]\right). \quad (10)$$

Although the essential non-zero part of the *C(n)* is located at the negative semi-axis, the *U(n)* function is seen in the positive semi-axis. Thus, it can be said that while the nucleation events usually occur at positive value of *n*, the value of *n* remains negative most of the time. Figure 2 shows the distribution as a function of the concentrations just before the nucleation event occurs (obtained from Eq. (10) for the same parameters as in Fig. 1 for different values of φ). As expected, the dispersion of *U(n)* is strongly controlled by the φ value and broadens very rapidly with decreasing φ. Since φ is proportional to R^{-3}, indicating that the temporal anti-correlation of nucleation events is more pronounced in thin NWs [10], leading to a more uniform length distribution [14].

III. Results and discussion

Equation (10) together with Eq. (4) allow us to calculate the distribution of the time intervals between the successive nucleation events, *T(x)*, using Eq. (5). This characteristic is the most important one, since it is directly related to the nucleation statistics as will be discussed shortly. Let us now consider the qualitative dependence of the *T(x)* shapes on some relevant parameters. In particular, Figures 3 show the radius dependences at $V = 4$ ML/s, $\tau = (R/R_0)\times 1s$, $b = (R/R_0)^2 \times 2\times10^5$ s^{-1}, $N_{eq} = (R/R_0)^3 \times 5\times10^6$, $M = (R/R_0)^2 \times 5\times10^4$,

$\varphi N_{eq} = 2\times10^3$, with $R_0 = 50$ nm and NW radii R varying from 12 to 500 nm. The values of N_{eq} and M must scale as R^3 and R^2, respectively. The droplet flux should be proportional to the surface area (R^2), while the effective lifetime τ scale with R to ensure that the desorption flux is proportional to R^2. In Fig. 3 (a), the *T(x)* distributions rapidly broaden with increasing R. Figure 3 (b) shows the relative standard deviation $\sigma_x / < x >$ as a function of the NW radius. Note that σ_x is (normalized to the mean value $< x >$ of the time interval between the two successive nucleations, which equals the inversed growth rate in ML/s. Both graphs reveal a transition from temporally anti-correlated to a Poissonian nucleation statistics, as discussed earlier [14].

While broadening of the *T(x)* distribution in thicker NWs is anticipated, the dependence on the desorption flux which was neglected in the literature [10, 14] is less obvious. Figures 4 show the *T(x)* profiles obtained at $V = 4$ ML/s, $M = 5\times10^4$, $N_{eq} = 5\times10^5$, $\varphi N_{eq} = 200$, $a = 2.5\times10^5$ s^{-1} and variable effective lifetimes τ, i.e., for a NW of a given radius exposed to a given vapor flux but with different desorption rates. The distributions presented in Fig. 4 (a) are shifted toward larger values for smaller τ, because an enhanced desorption leads to a lower mean growth rate of a NW. More importantly, it is seen that higher desorption rates correspond to broader distributions of the nucleation events, i.e. the desorption works against the temporal anti-correlated nucleation statistics. This new effect is also well illustrated by the curve in Fig. 4 (b), where the relative standard deviation $\sigma_x / < x >$ rapidly increases towards smaller τ, starting from $\tau \cong 0.3$ s, while it is almost constant for $\tau > 0.5$ s with our model parameters.

Let us now consider the experimental data on Au-catalyzed Si NWs. [24], where the oscillatory length-time dependence was obtained by *in situ* monitoring of VLS growth in an ultrahigh vacuum transmission electron microscope. From these data, the histograms of the

time intervals between the successive nucleations extracted are shown in Figs. 5 for three samples grown at the same temperature of 480°C but with different Si_2H_6 partial pressures. The NW diameter was set to 15 nm based on the TEM images [24]. The growth temperature of 480°C corresponds to ~24% equilibrium Si concentration in the droplet [32]. This yields the values of N_{eq}=43100 and M=5600 for our model parameters. The average growth rates, also measured from the plots given in [24], were estimated to be 0.75, 1.25 and 1.5 ML/s for the Si_2H_6 partial pressure of 2.0×10^{-6}, 4.0×10^{-6} and 5.0×10^{-6} Torr, respectively.

The effective lifetime of Si atoms is then set to a plausible value of τ=1 s. After that, the values of φ and b were adjusted to obtain the fits shown by lines in Figs. 5. The fitting values are summarized in Table 1, showing that the φ value decreases and the b value increases with the growth rate. Figures 5 demonstrate that, while the mean time interval between the successive nucleation events decreases with the partial pressure of Si_2H_6, the relative width of nucleation distributions increases towards a higher growth rate, the effect noticed elsewhere [14]. Overall, the fits obtained are fairly good given the scatter in the experimental data.

Table 1. Parameter values for Si NWs grown at different partial pressures of Si precursor

Si_2H_6 partial pressures	Growth rate	φ	b
2×10^{-6} Torr	0.75 ML/s	$2.32\text{x}10^{-3}$	2690 s^{-1}
4×10^{-6} Torr	1.25 ML/s	$1.28\text{x}10^{-3}$	5040 s^{-1}
5×10^{-6} Torr	1.5 ML/s	$1.04\text{x}10^{-3}$	5600 s^{-1}

In Ref. [10], by post-growth measurements of Au-catalyzed InPAs NWs with modulated composition [11], the authors found a sub-Poissonian character of the nucleation statistics. This results in narrowing the experimental histogram of the numbers of nucleation events per composition oscillation, Fig. 6 [10]. In order to fit these data by our model, we use the equation

$$N_\delta(m) = T\left(\frac{\delta}{m}\right)\frac{\delta}{m^2}, \tag{11}$$

where the left hand side is the number of composition oscillations with a given duration δ, and m is the number of MLs per oscillation. The best fit is shown by line in Fig. 4, with the parameters summarized in the figure caption.

We note that while the fits to the experimental data in Figs. 5 and 6 are very reasonable, which supports our model, the shapes of nucleation distributions are strongly influenced by the parameter φ which is hard to determine independently. Also, additional studies are required in order to determine the temperature-dependent desorption fluxes from liquid droplets, which would help to eliminate the uncertainty in τ.

In summary, we have developed a model describing the time distribution of the nucleation events during the VLS growth of NWs. The model accounts for desorption from the droplet and allows one to describe the nucleation statistics and the NW length distribution. It was shown that the relative dispersion of nucleation distribution over time increases with the NW radius and at a higher desorption from the droplet. It was also demonstrated that reasonably good fits to the available experimental data on the nucleation statistics in both III-V and Si VLS NWs were achieved.

Acknowledgement

This work was partially supported by the grants of the Russian Foundation for Basic Research, contracts with the Russian Ministry of Education and Science, scientific programs of the Russian Academy of Sciences, and the FP7 projects NANOEMBRACE (316751), SOBONA (268154) and FUNPROB (269169). We wish to thank Frank Glas for discussing the importance of nucleation statistics in VLS NWs, and for explaining his own modeling results on this subject. N.V.S. acknowledges the financial support from the Council on Grants of the President of the Russian Federation.

References

[1] Y. Cui and C. M. Lieber, Science 91, (2001) 851.

DOI: 10.1126/science.291.5505.851

[2] B. O. Jung, Y. H. Kwon, D. J. Seo, D. S. Lee, H. K. Cho Journal of Crystal Growth 370 (2013) 314

DOI: 10.1016/j.jcrysgro.2012.10.037

[3] J. Teubert, P. Becker, F. Furtmayr and M Eickhoff Nanotechnology 22 (2011) 275505

DOI: 10.1088/0957-4484/22/27/275505

[4] P. Tovee, M.E. Pumarol, D.A. Zeze, K. Kjoller, O. Kolosov Journal of Applied Physics, 112 (2012) 114317.

DOI: 10.1063/1.4767923

[5] E.I. Givargizov, Journal of Crystal Growth 31 (1975) 20

DOI: 10.1016/0022-0248(75)90105-0

[6] V.G.Dubrovskii, N.V.Sibirev, Physical Review E, 70 (2004) 031604

DOI: 10.1103/PhysRevE.70.031604

[7] F. Glas, J. C. Harmand, and G. Patriarche, Physical Review Letters 99 (2007) 146101

DOI: 10.1103/PhysRevLett.99.146101

[8] V.G. Dubrovskii and N.V. Sibirev Journal of Crystal Growth, 304 (2007) 504

DOI: 10.1016/j.jcrysgro.2007.03.034

[9] B. A. Wacaser, K.A. Dick, J.Johansson, M. T. Borgström, K. Deppert, and L. Samuelson Advanced Materials 21 (2009) 153

DOI: 10.1002/adma.200800440

[10] F. Glas, J.C. Harmand, G. Patriarche, Physical Review Letters 104 (2010) 135501

DOI: 10.1103/PhysRevLett.104.135501

[11] J.C. Harmand, F. Glas, G. Patriarche, Physical Review B 81, (2010) 235436

DOI: 10.1103/PhysRevB.81.235436

[12] P. Krogstrup, S. Curiotto, E. Johnson, M. Aagesen, J. Nygard, D. Chatain Physical Review Letters 106, (2011) 125505

DOI: 10.1103/PhysRevLett.106.125505

[13] R. T. Tucker, A. L. Beaudry, J. M. LaForge, M. T. Taschuk, M. J. Brett Applied Physics Letters 101 (2012) 193101

DOI: 10.1063/1.4764508

[14] V. G. Dubrovskii, Physical Review B 87 (2013) 195426

DOI: 10.1103/PhysRevB.87.195426

[15] P. Krogstrup, H. I Jørgensen, E. Johnson, M. H. Madsen, C. B. Sørensen, A. Fontcuberta i Morral, M. Aagesen, J. Nygård, F. Glas Journal of Physics D- Applied Physics. 46, (2013), 313001

DOI: 10.1088/0022-3727/46/31/313001

[16] F. M. Ross, J. Tersoff, and M. C. Reuter, Physical Review Letters 95, (2005) 146104

DOI: 10.1103/PhysRevLett.95.146104

[17] V.G. Dubrovskii, N.V. Sibirev, G.E. Cirlin, J.C. Harmand, V.M. Ustinov, Physical Review E 73, (2006) 021603

DOI: 10.1103/PhysRevE.73.021603

[18] V.G. Dubrovskii, T. Xu, Y. Lambert, J.-P. Nys, B. Grandidier, D. Stievenard, W. Chen, P. Pareige, Physical Review Letters 108, (2012) 105501

DOI: 10.1103/PhysRevLett.108.105501

[19] N.V. Sibirev, M.A. Timofeeva, A.D. Bol'shakov, M.V. Nazarenko, and V.G. Dubrovskii Physics of the Solid State, 52(7) (2010) 1531

DOI: 10.1134/S1063783410070309

[20] T. Chiaramonte, L. H. G. Tizei, D. Ugarte, M. A. Cotta, Nano Letters 11 (2011) 1934
DOI: 10.1021/nl200083f

[21] L. Rigutti, A. D. L. Bugallo, M. Tchernycheva, G. Jacopin, F. H. Julien, G. Cirlin, G. Patriarche, D. Lucot, L. Travers, J.-C. Harmand J. Nanomaterials (2009) 435451
DOI: 10.1155/2009/435451

[22] W. Chen, V.G. Dubrovskii, X. Liu, T. Xu, R. Larde, J. P. Nys, B. Grandidier, D. Stievenard, G. Patriarche, and P. Pareige, Journal of Applied Physics 111, (2012) 094909
DOI: 10.1063/1.4714364

[23] C.-Y. Wen, J. Tersoff, M.C. Reuter, E.A. Stach, and F.M. Ross, Physical Review Letters 105 (2010) 195502
DOI: 10.1103/PhysRevLett.105.195502

[24] C.-Y. Wen, J. Tersoff, K. Hillerich, M. C. Reuter, J. H. Park, S. Kodambaka, E. A. Stach, F. M. Ross Physical Review Letters 107 (2011) 025503
DOI: 10.1103/PhysRevLett.107.025503

[25] N.V.Sibirev and V.G.Dubrovskii Technical Physics Letters 30(9), (2004), 791
DOI: 10.1134/1.1804598

[26] S.H. Oh, M. F. Chisholm, Y. Kauffmann, W. D. Kaplan, W. Luo, M. Rühle, and C. Scheu, Science 330 (2010) 489
DOI: 10.1126/science.1190596

[27] D. Kashchiev, Crystal Growth & Design 6, (2006) 1154
DOI: 10.1021/cg050619i

[28] J. Johansson, L. S. Karlsson, K. A. Dick, J. Bolinsson, B. A. Wacaser, K. Deppert, and L. Samuelson, Crystal Growth & Design 9, (2009) 766
DOI: 10.1021/cg800270q

[29] N.V. Sibirev Technical Physics Letters 39(7) (2013) 77

DOI: 10.1134/S1063785013070237

[30] A. D. Gamalski, C. Ducati, S. Hofmann, Journal of Physical Chemistry C 115 (2011) 4413.

DOI: 10.1021/jp1095882

[31] R. Bellman, K. L. Cooke, Differential-Difference Equations. New York/London, Academic Press,1963.

[32] T. B. Massalski, Binary Alloy Phase Diagrams (Metals Park, OH: ASM International), 1986

Figure Captions:

Fig. 1. Probabilities $C(n)$ to observe $N_* + n$ semiconductor atoms in the droplet at different φ .

Fig. 2. Distributions over concentration $U(n)$ just before the nucleation event at different φ .

Fig. 3. (a) Time dependence of the delays between the successive nucleation events $T(x)$ in NWs as a function of the radius R ; (b) Radius dependence of the normalized standard deviation $\sigma_x / < x >$.

Fig. 4. (a) Time dependence of the delays between the successive nucleation events $T(x)$ in NWs with different life times τ ; (b) Dependence of the normalized standard deviation $\sigma_x / < x >$ on τ . The solid line in (b) represents the best fit ($0.0134/[\tau(\tau - 0.1)]^{3/4} + 0.09$).

Fig. 5. Histograms of the time intervals between the successive nucleations, extracted from the data of Ref. [24] for three samples grown at Si_2H_6 partial pressures of 2×10^{-6} (a), 4×10^{-6} (b) and 5×10^{-6} Torr (c) (bars), fitted by theoretical curves (lines) with the parameters summarized in Table 1.

Fig. 6. Experimental histogram of the numbers of nucleation events per composition oscillation from Ref. [10] (bars), fitted by Eq. (11) (line) with the following parameters: δ=3.6 s, V=3ML/s, φ=4x10^{-4}, b=2.4x10^5 s^{-1}, M=5x10^4, τ=1 s.

Figure 1

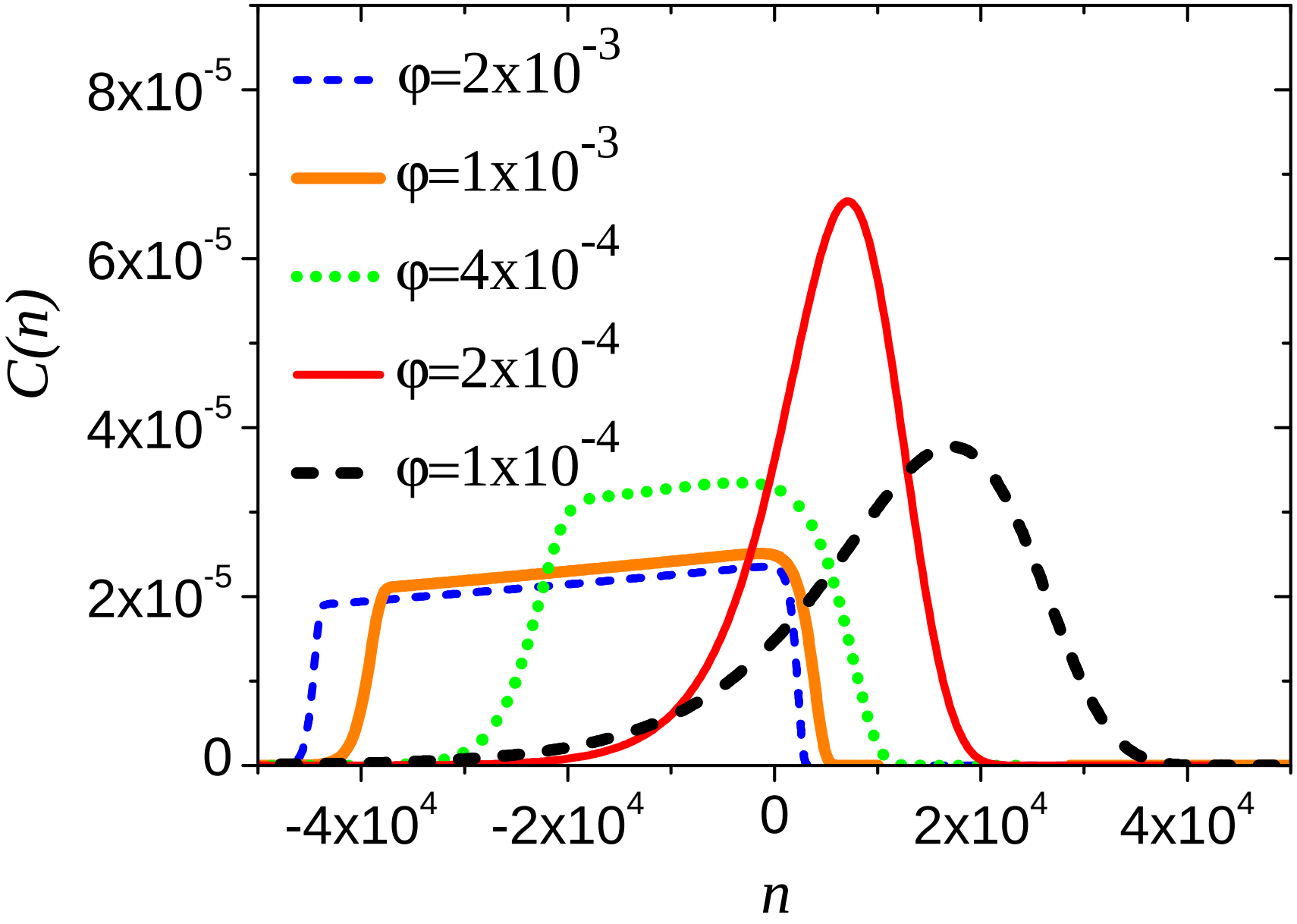
φ=2x10^-3
φ=1x10^-3
φ=4x10^-4
φ=2x10^-4
φ=1x10^-4
8x10^-5
6x10^-5
4x10^-5
2x10^-5
0
C(n)
-4x10^4
-2x10^4
0
2x10^4
4x10^4
n

Figure 2

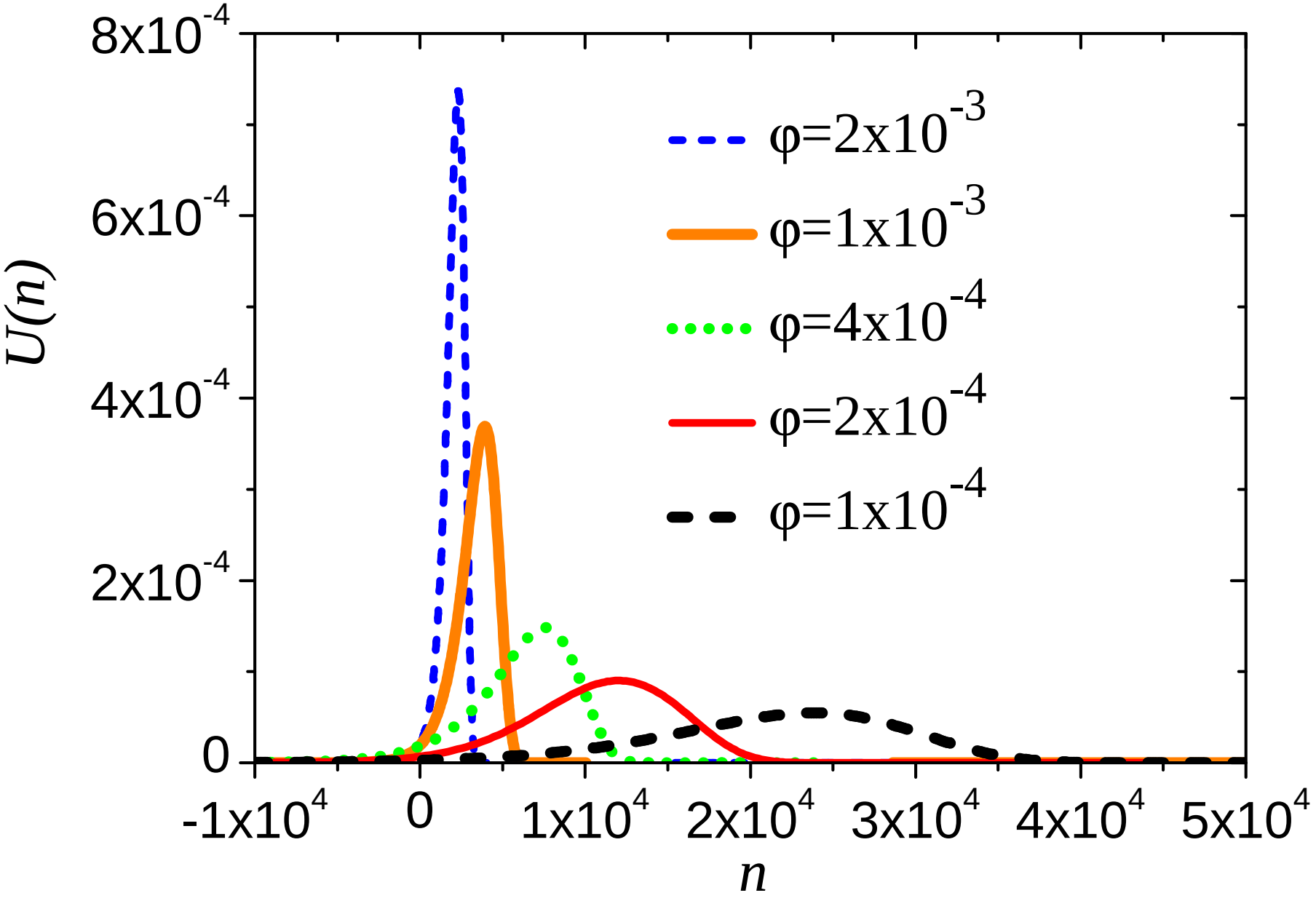
8x10^-4
6x10^-4
4x10^-4
2x10^-4
0
U(n)
-1x10^4
0
1x10^4
2x10^4
3x10^4
4x10^4
5x10^4
n
φ=2x10^-3
φ=1x10^-3
φ=4x10^-4
φ=2x10^-4
φ=1x10^-4

Figure 3a

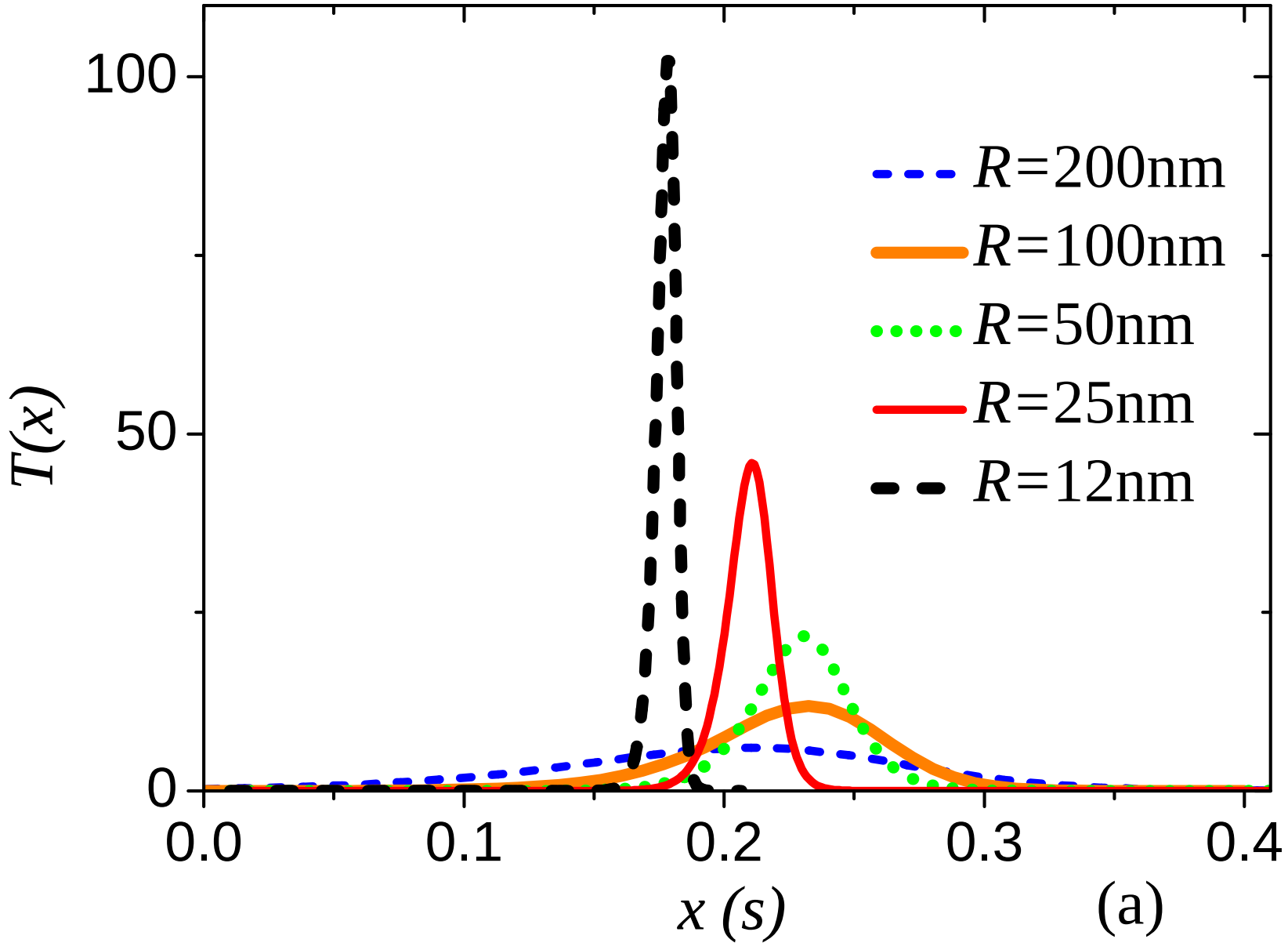

Figure 3b

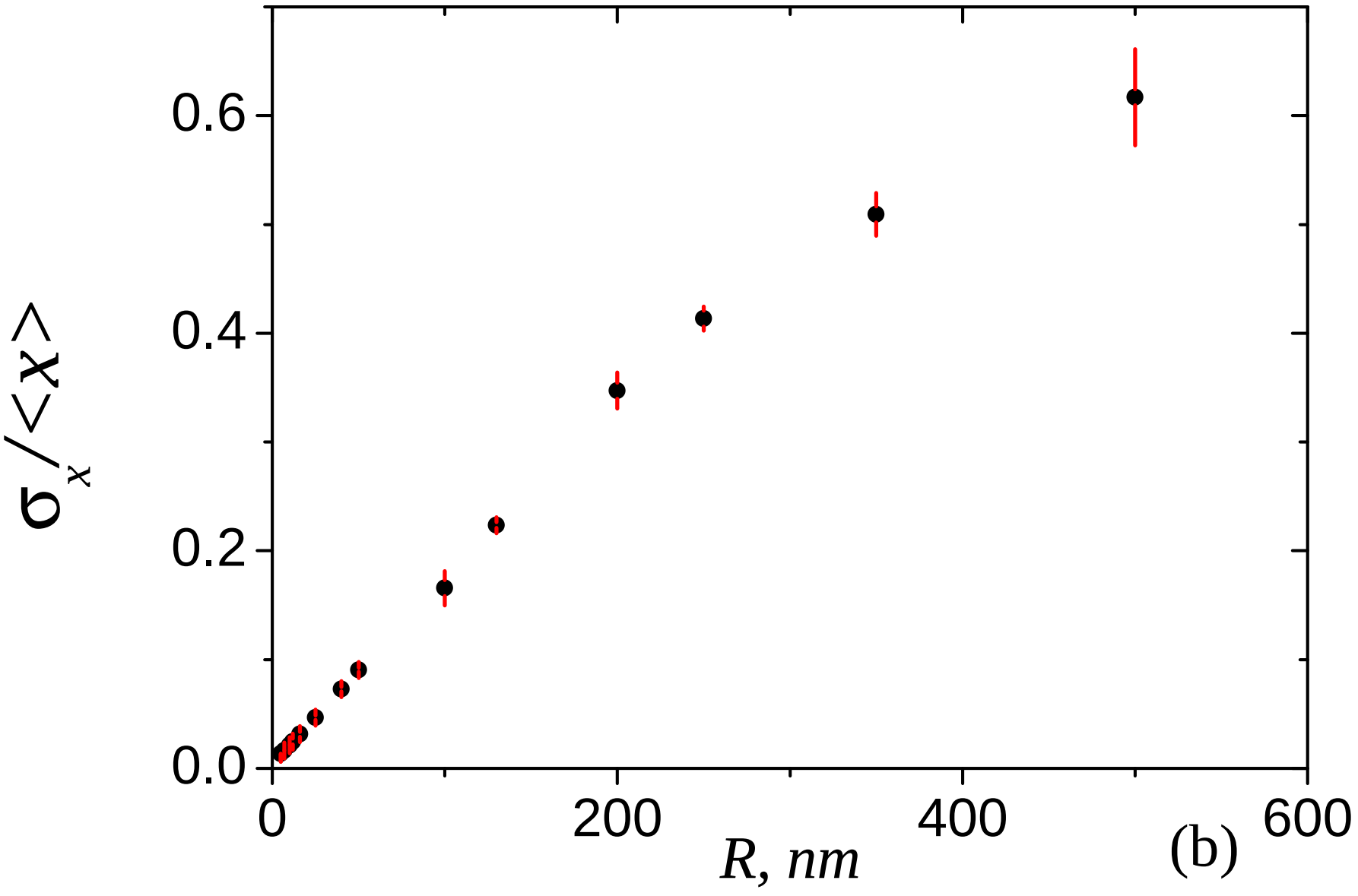

Figure 4a

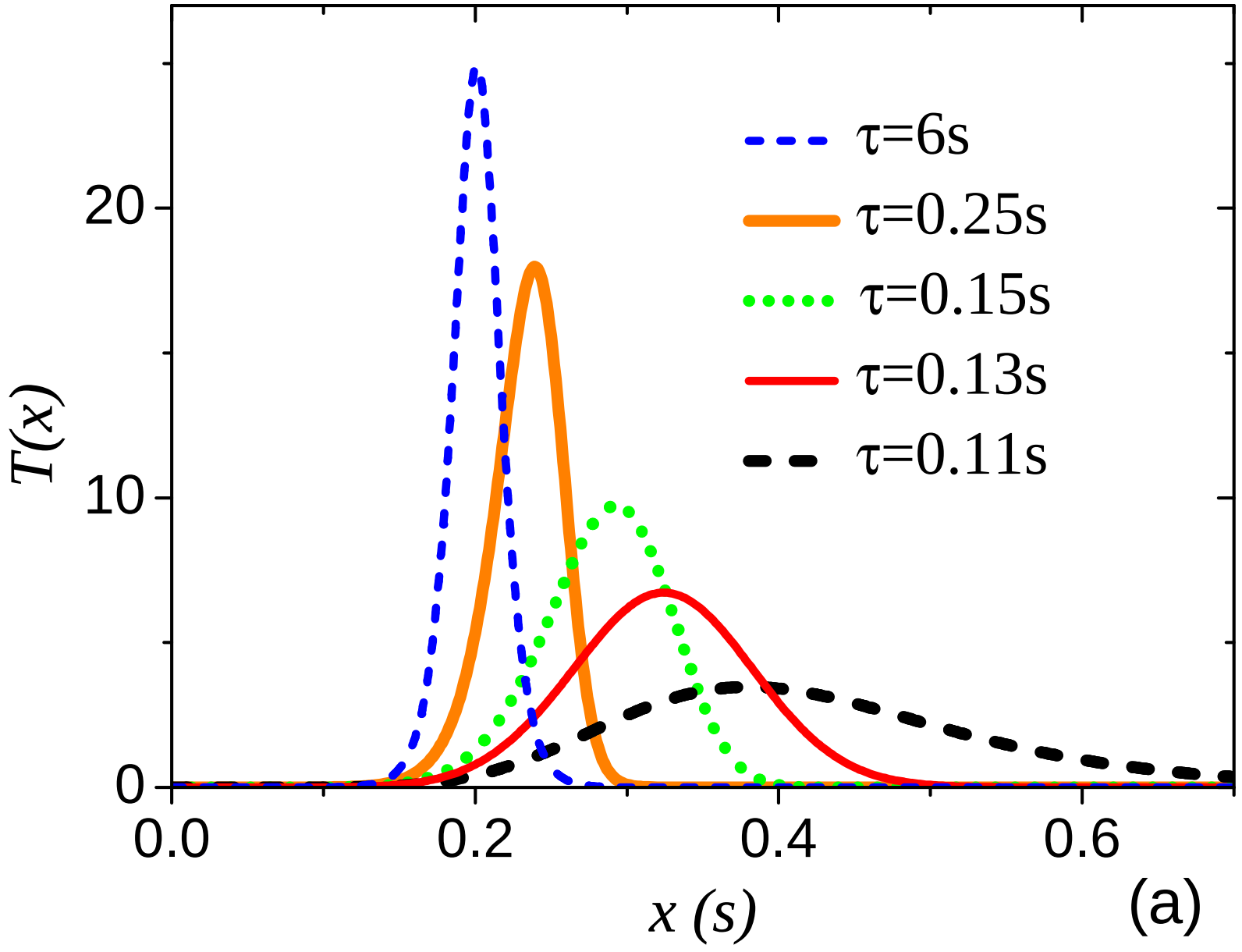

Figure 4b

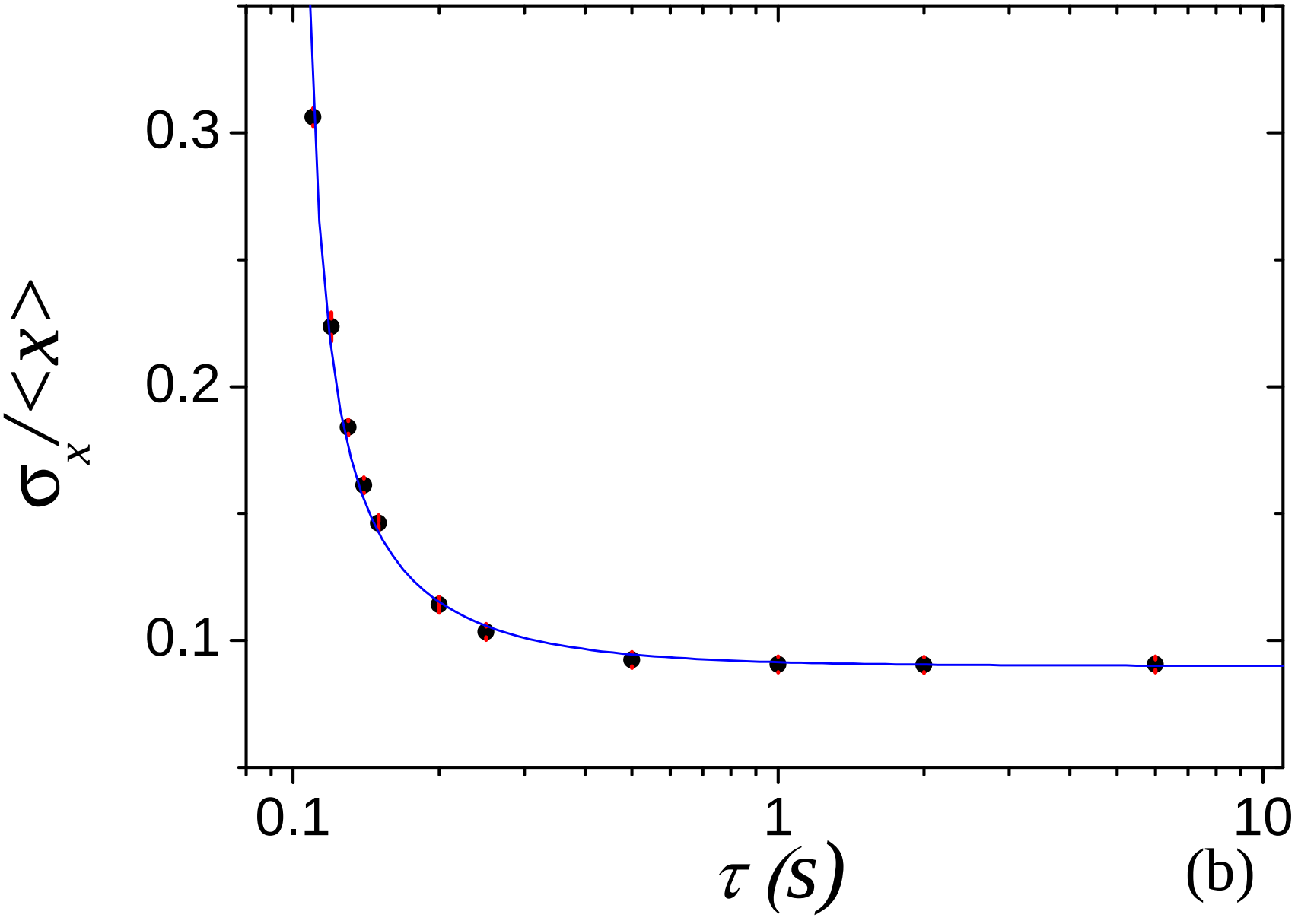

Figure 5a

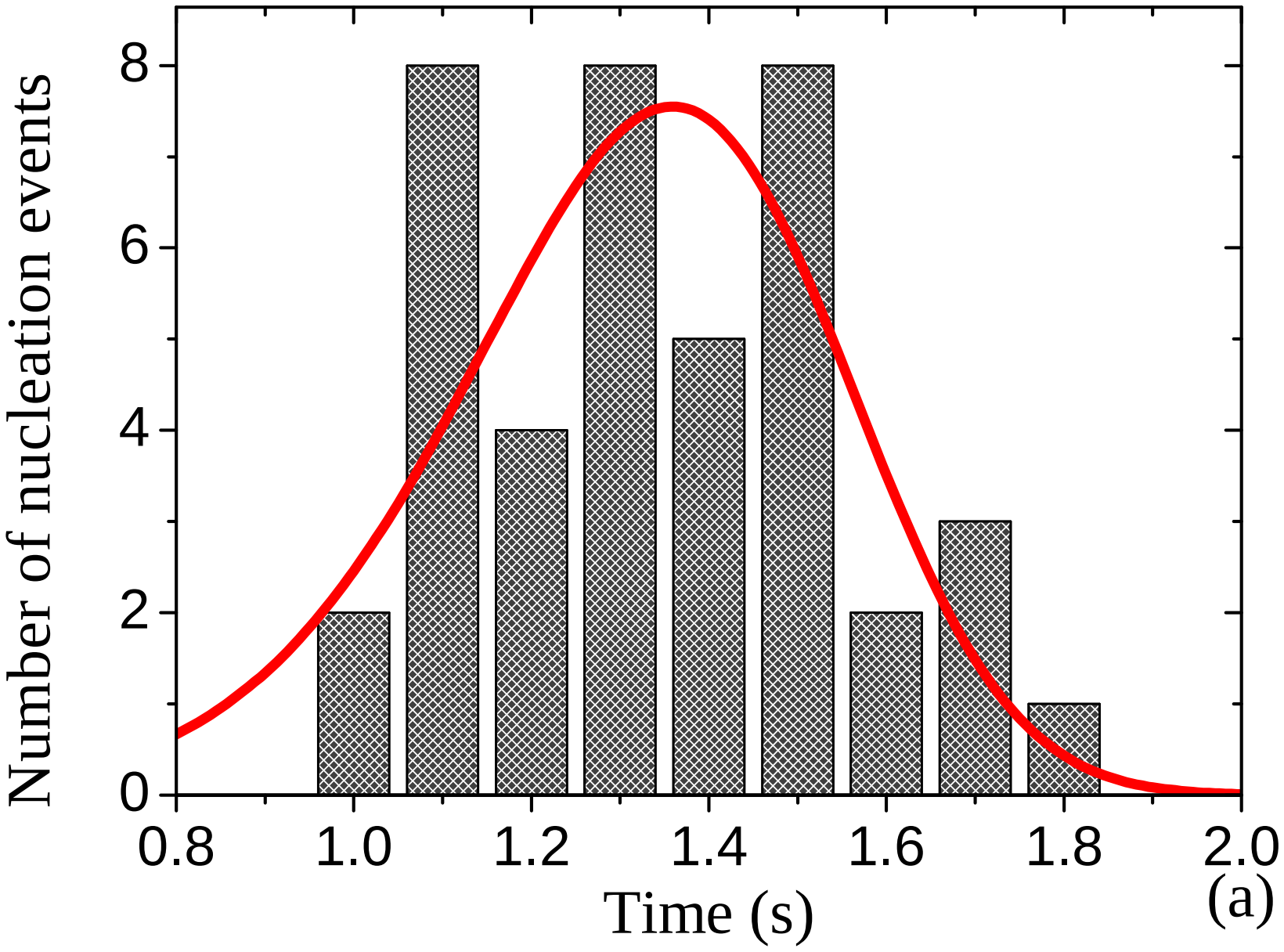

Figure 5b

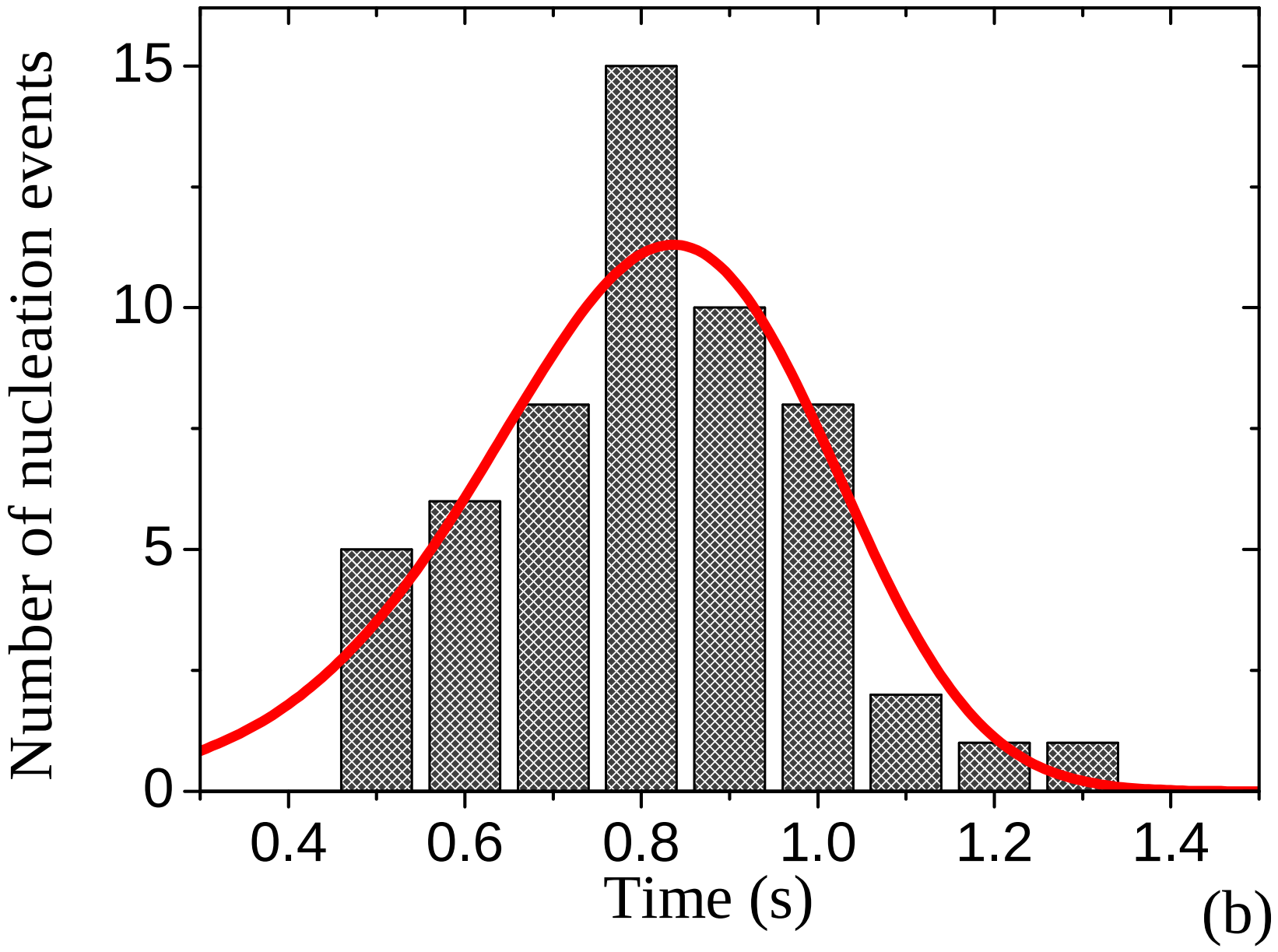

Figure 5c

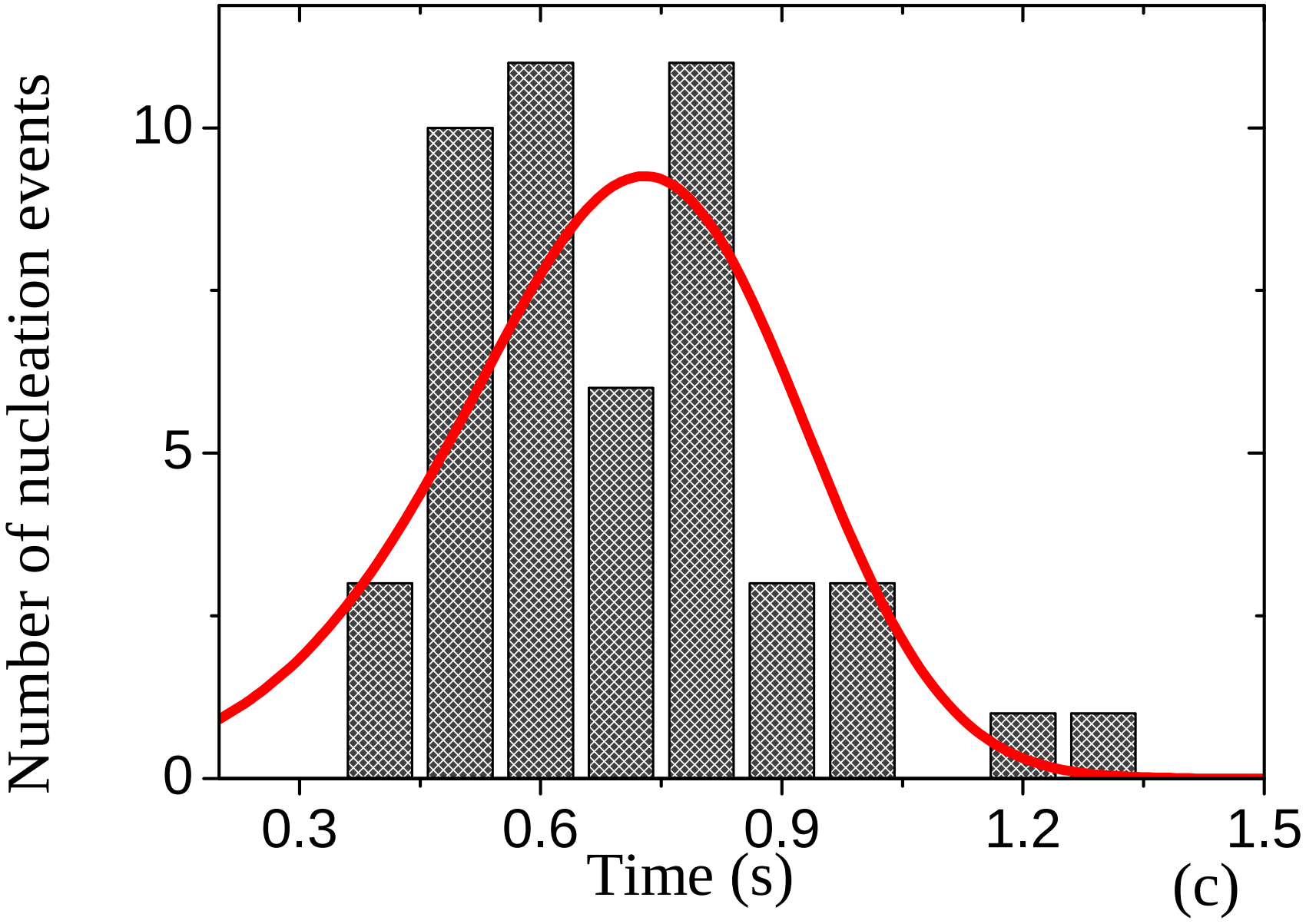

Figure 6

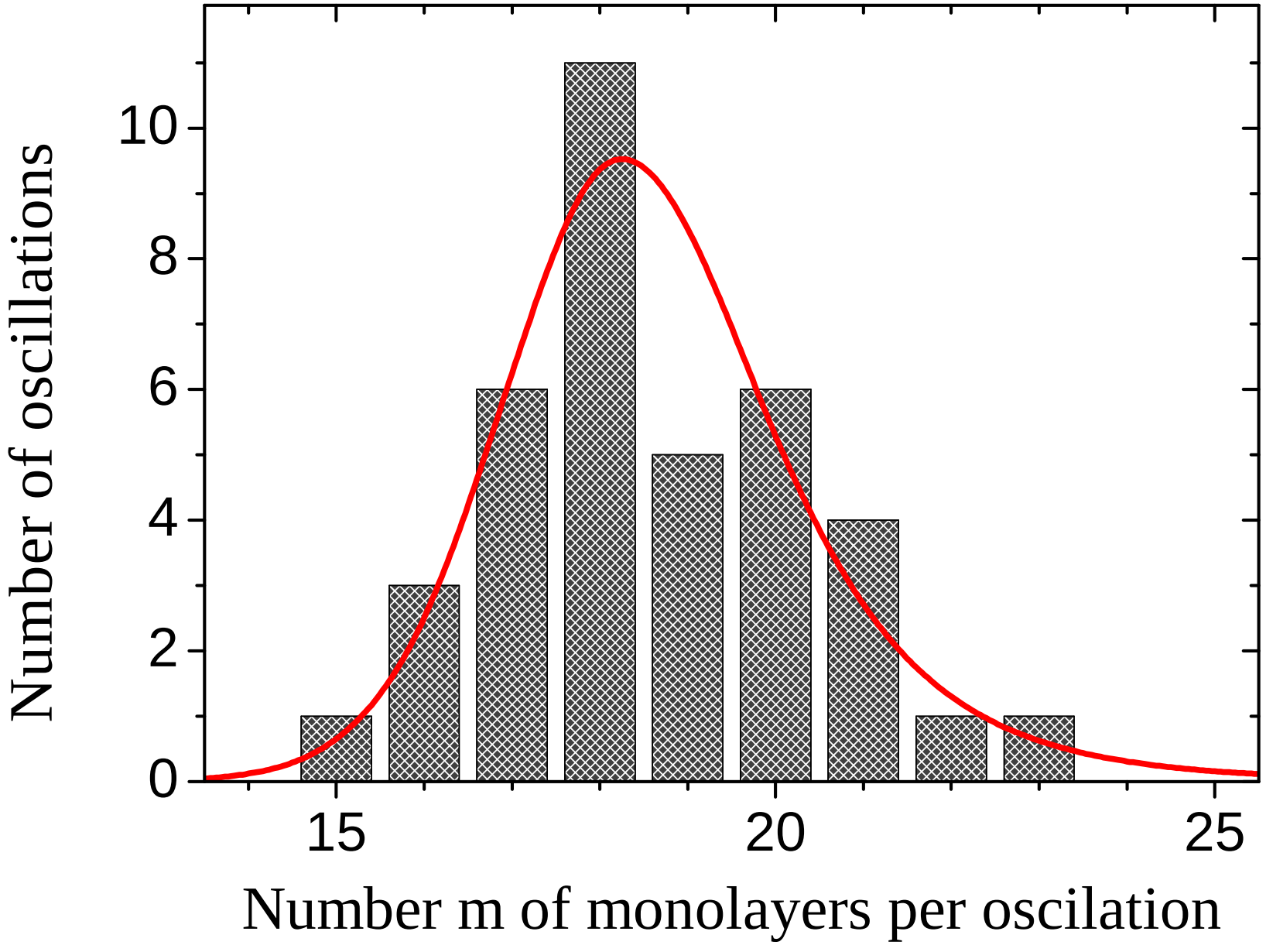
Number of oscillations
0
2
4
6
8
10
15
20
25
Number m of monolayers per oscilation